

# Molecular Dynamics of DNA Origami Nanostructures

*Annual Report for  
Blue Waters Allocation*

Aleksei Aksimentiev – Principal Investigator

January 23, 2015

Center for the Physics of Living Cells  
Department of Physics  
University of Illinois at Urbana-Champaign

## Executive summary

DNA origami is a rapidly emerging technology that enables high-throughput construction of DNA-based sub-micron-size nanomachines with nanoscale accuracy. Similar to the computer-aided design (CAD) of the real-world machines (e.g., airplanes), our group is pioneering CAD for nanoscale machines made of DNA origami. To achieve accuracy high enough to predict both chemical and mechanical properties of DNA origami objects, we employ all-atom molecular dynamics (MD) simulations. Blue Waters supercomputer was essential for achieving this goal due to sheer size of the DNA origami objects and computationally demanding nature of MD technique. In this report, we present our achievements using the JQ5 allocation for the year of 2014. Our achievements include MD simulations of sub-micron-size DNA sculpture, characterization of electric properties of DNA nanoplates and biomimetic DNA nanochannels. Comparison of our results with experimental data demonstrates that the predictive design of DNA origami on Blue Waters will be possible in the near future.

# Description of research activities and results

## Key challenges

Self-assembly of DNA into complex three-dimensional objects has emerged as a new paradigm for practical nanotechnology [1, 2]. Among the methods that have been put forward that utilize self-assembly of DNA [2], DNA origami [3] stands out through its conceptual simplicity and infinite range of possible applications [1, 2]. The basic principle of DNA origami is the programmed folding of a long (tens of thousands of nucleotides) DNA strand into a custom two- or three-dimensional (3D) shape, guided by specially designed short oligonucleotides [3]. Since its first demonstration in 2006, the DNA origami method has advanced to encompass self-assembly of complex 3D objects with sub-nanometer precision [4] including static structures [5, 6, 1, 2] as well as objects that perform active functions [7, 8, 9]. Recent methodological advances [10] have made practical applications [10, 11, 12, 13] of DNA origami feasible.

Experimental characterization of DNA origami is essential for accurate design, but has been limited to rather qualitative techniques such as atomic force spectroscopy [7], small-angle X-ray scattering [7], and transmission electron microscopy [5, 4]. Recently, super-resolution optical imaging [9], fluorescence resonance energy transfer (FRET) [12] and magnetic tweezers [14] have been applied to DNA origami objects to infer information about their *in situ* structure and dynamics. The only atomic-level model of DNA origami *in situ* has been derived from cryo-electron microscopy (cryo-EM) [15], which revealed considerable deviations from the idealized design. Here, we describe our ongoing efforts to develop a computational approach that can replace the experimental characterization procedure to facilitate novel DNA origami designs that function as desired.

## Why it Matters

Predictive computational modeling of DNA origami objects is an attractive alternative to experimental characterization procedures, which are expensive and time-consuming. It is already common practice for experimentalists to use the simplest available computational description of DNA—a continuum-based model—to validate their designs [16, 17]. In these models, DNA double helices are approximated as uniform cylinders with material properties set to reproduce the average bending rigidity of DNA helices. Unfortunately, this level of description permits only semi-quantitative estimation of the overall structure [17]. There are also several coarse-grained models of DNA that are more sophisticated than continuum-based models and can represent the double-helical structure of DNA [18, 19, 20]. In a typical coarse-grained DNA model, each nucleotide is represented by 2–3 interaction beads. When the interaction parameters are properly optimized, such models have the potential to make realistic predictions. However, these models are new and their accuracy is not well-established.

Currently, the most accurate computational method that can realize our goal—prediction of structure and function of DNA origami objects—is the all-atom molecular dynamics (MD) method. In 2013, we reported the first MD simulations of several model DNA origami systems [21]. Our simulation results were in exceptional agreement with the experimentally

determined structural characteristics, proving the unmatched accuracy of the MD approach. Since then, we have been trailblazing the application of the MD method to DNA origami objects by investigating various real-world problems. The systems we have been simulating include a sub-micron-size sculpture with nano-meter-scale precision, a nano-plate for the design of nano-scale sensors, a nano-scale box for drug delivery, and bio-mimetic nanochannels. The current status of these projects is summarized in the Accomplishments section. Based on these studies, we will develop MD-simulation protocols for a predictive modeling of DNA origami objects. Moreover, we will demonstrate utility of the MD simulation technique to design novel DNA origami systems.

## Why Blue Waters

DNA origami nanostructures can be as large as 30 nm [11, 15, 7]. Although rough estimation of their structures can be done using simpler models [16], accurate prediction of structure requires all-atom approach [21]. Furthermore, all-atom MD simulation is the only computational method that can treat DNA origami objects enhanced by non-standard functional groups. For example, all-atom MD simulation is the only method that can characterize the transport phenomena in simulations of DNA origami channels or nanoplates.

All-atom simulations of large-scale DNA origami objects including explicit treatment of water molecules require powerful computational resources. Through the past year, we demonstrated that the Blue Waters supercomputer is ideal for simulations of large-scale DNA origami objects.

## Accomplishments

Using 240,000 node-hour allocations (JQ5 project), we performed three large-scale MD simulations of DNA origami. First, we have used our MD method to measure the ionic conductivity of DNA origami plates [22] (Section A1). A manuscript based on this work is under revision in the journal *ACS Nano* (impact factor 12). Our simulations predicted that the conductivity of DNA origami plates depends on their orientation (Section A1.1) and the concentration of magnesium ions in solution (Section A1.2). These predictions were experimentally verified through nano-capillary ionic current recordings and FRET measurements [22]. We have shown that DNA origami plates can deform in an electric field as a result of competing electrophoretic and electroosmotic forces (Section A1.3). Second, direct comparison of the MD predictions with the results of cryo-EM reconstruction [15] have validated the structural models emerging from the MD simulations (Section A2). Third, we have carried out the first simulations of DNA origami ion channels that have elucidated the structural origin of the leakage current and its dependence on the channel architecture (Section A3). We have also used a part of last year allocation to complete several projects that were started using XSEDE allocation [23, 24, 25, 26]

### **A1. Ionic conductivity of DNA origami plates.**

In a typical simulation of DNA origami plates, a fragment of a DNA origami plate was submerged in electrolyte solution and subjected to an external electric field, which produced a drop in electrostatic potential across the plate, Fig. 1a. The current of ions produced by the electric field was determined by summing up ion displacements over the simulation system

and the MD trajectory [27]. Repeating the simulations for different designs of the DNA origami plates determined the dependence of the plates' ionic conductivity on the number of DNA layers, the lattice type and the nucleotide content. The ionic current was found to be carried predominantly (80~85%) by potassium ions; the current–voltage dependence was slightly non-linear.

**A1.1. Anisotropy.** DNA origami is an intrinsically anisotropic material, so its conductance depends on the direction of the applied electric field, Fig. 1c. We have assessed the degree of such anisotropy by simulating ionic current through a fragment of a DNA origami plate in three different directions. Our simulations predicted the conductivity of a square-lattice DNA origami plate to be the largest in the direction of the DNA helices, Fig. 1d. To confirm our predictions, the Keyser group (Cambridge, UK) designed a set of DNA origami structures whose orientation with respect to the applied electric field could be controlled. Ionic current measurements carried out on such systems directly confirmed our predictions [22].

**A1.2. Effect of divalent ions.** MD simulations of ionic current performed at different concentrations of  $\text{Mg}^{2+}$  ions revealed a linear anti-correlation between  $\text{Mg}^{2+}$  concentration and the conductance of the DNA origami plate, Fig. 1e. Further analysis revealed that the anti-correlation is caused by the compaction of the DNA origami structure Fig. 1e. Thus, increasing the concentration of  $\text{Mg}^{2+}$  ions makes the DNA origami plate more compact, de-

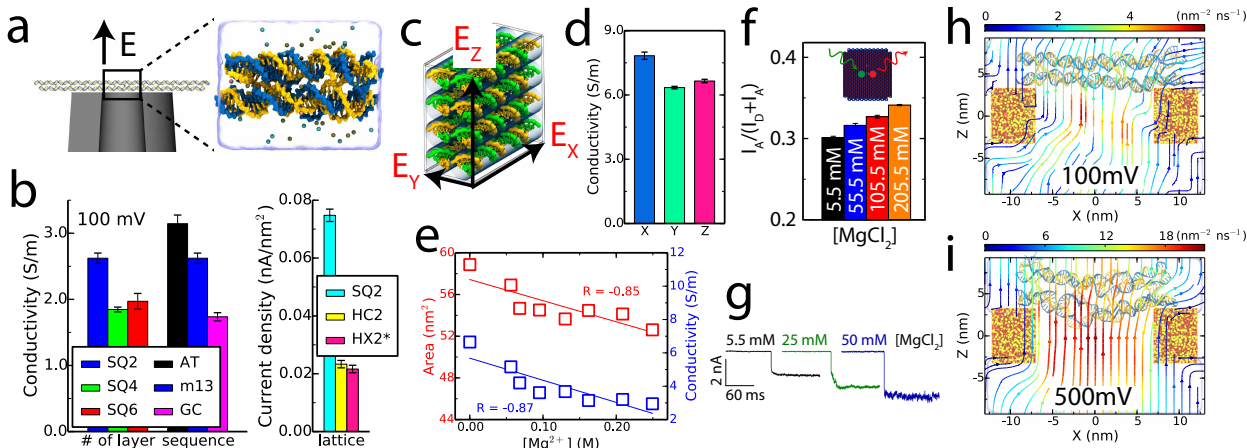


Figure 1: MD simulations of DNA origami conductivity (a) Schematic of the experimental setup (left). All-atom model of the experimental system (right) containing scaffold (blue) and staple (yellow) strands, water (semitransparent molecular surface) and ions (spheres). (b) Ionic conductivity of the DNA origami plate depends on the number of DNA layers (2, 4 or 6) and on the nucleotide composition poly(AT), m13 viral DNA, and poly(GC) (left). The ionic current density through the plate depends on the packing type of the DNA helices (right). SQ2, HC2 and HX2\* denote 2-layer square-lattice, honeycomb and hexagonal DNA origami plates. (c,d) Anisotropic conductivity of a DNA origami plate. Schematic of the simulation setup (c) and the simulated conductivity along the  $x$ ,  $y$  and  $z$  axes (d). (e) Simulated dependence of the plate's area (left axis) and ionic conductivity (right axis) on bulk concentration of  $\text{Mg}^{2+}$ . (f) FRET efficiency from a pair of Cy3–Cy5 dyes versus  $\text{MgCl}_2$  concentration. The horizontal axis is not drawn to the scale. The data indicate compaction of the DNA plate with increasing  $\text{Mg}^{2+}$  concentration. (g) Experimental dependence of the ionic current through a DNA origami plate on  $\text{MgCl}_2$  concentration. (h,i) Structural deformation of a DNA origami plate on top of a  $\text{SiO}_2$  nanogap after 100 ns of MD simulation. The streamlines illustrate the magnitude of the local water flux.

creasing its conductivity. These predictions were directly confirmed by measurements of the FRET intensity from the two dyes incorporated within the DNA origami structure, Fig. 1f, and by measurements of the ionic current blockades produced by the presence of a DNA origami plate on top of a nano-capillary, Fig. 1f, as a function of magnesium concentration. These results demonstrate the predictive power of the all-atom MD method in characterizing the ionic conductivity of DNA origami plates.

**A1.3. Deformability.** Being negatively charged, a DNA origami plate moves in an external electric field, loading itself on top of a nanocapillary or a solid-state nanopore [28, 29, 30, 31]. Once placed on a solid-state support, the motion of the plate is arrested; however, further deformation of the internal structure can occur under the action of the electric field. Our preliminary MD simulations identified two types of structural deformations caused by the applied electric field [22]: the plate was observed to both expand and bend, Fig. 1h,i. Analysis of the MD trajectories revealed that such deformations are caused by the competition of the electrophoretic force pulling the DNA plate into the gap and the hydrodynamic drag of the electroosmotic flow [32] forcing the layers of the plate to come apart. The simulations also provided a detailed account of the voltage dependence of the DNA origami plate’s conductivity, elucidating the role of structural deformation [22].

**A2. Direct comparison with the results of cryo-EM reconstruction.**

The cryo-EM method has been used to obtain the most detailed experimental characterization of the *in situ* structure of a DNA origami object [15]. The system used for the study contained 5,238 nucleotides in 82 dsDNA helices and included various types of connections commonly found in DNA origami objects. To test the accuracy of our MD method, we have begun a fully atomistic explicit solvent MD simulation of the exact DNA origami design characterized with the cryo-EM method. The caDNAno design provided by Bai *et al.* was converted to an all-atom representation, Fig. 2a(i). As of the writing of this proposal, the simulation has run for almost 50 ns; from which only the first 5 ns was restrained equilibration. The conformation of the structure at this stage of the simulation is shown in Fig. 2a(ii), and for comparison, the 3D reconstruction of the experimental structure from cryo-EM measurements is shown in Fig. 2a(iii). Note that due to the limited resolution of the cryo-EM model, the ssDNA strands visible in the all-atom representations could not be reconstructed using cryo-EM measurements. The conformational change of the structure

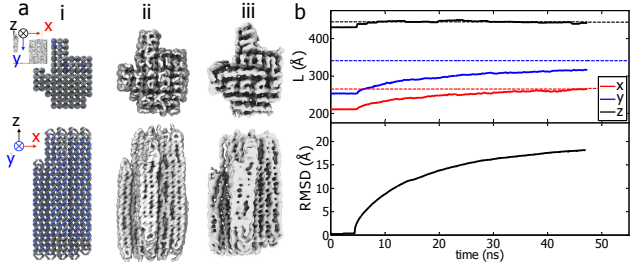


**Figure 2:** Comparison of all-atom MD simulation of a large DNA origami structure with cryo-EM reconstruction. (a) Comparisons of the structural models. (i) Orthogonal views of the idealized design. (ii) Orthogonal views of the design after  $\sim 50$  ns of explicit solvent MD simulation. (iii) Orthogonal views of the cryo-EM reconstruction [15]. (b) Changes in the DNA origami structure during MD simulation.

(Top) The length of the structure, not including ssDNA strands, in the specified dimension  $L$  is plotted versus simulation time; dashed lines indicate the value obtained from the cryo-EM model. (Bottom) The root mean square deviation of the atomic coordinates from their initial values versus simulation time.

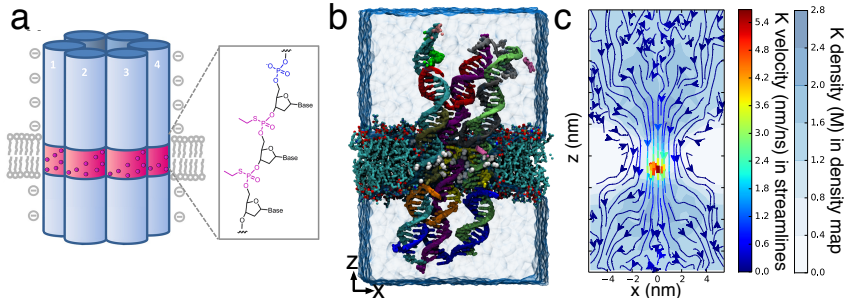


**Figure 3:** DNA origami membrane channel. (a) Schematic design of the DNA channel used for ionic current measurements [33]. The channel consists of six DNA helices modified to incorporate hydrophobic ethylthiolate moieties for anchoring to a lipid bilayer [33]. (b) An

equilibrated model of the DNA channel obtained by MD simulation. For clarity, the image explicitly shows only three out of six DNA helices. (c) The average density and local flux of  $K^+$  ions obtained from MD simulation at a transmembrane bias of 200 mV.

throughout the simulation was monitored by both calculating the root mean square deviation (RMSD) between the idealized conformation and the conformation at a given time, and measuring the structure’s dimensions ( $L$ ) along the  $x$ ,  $y$ , and  $z$  axes over time, Fig. 2b. Although the structural relaxation is not yet complete, the size of the simulated structure steadily approaches the size captured in the cryo-EM structure, while large scale deformations similar to those captured in the cryo-EM structure emerge. At the same time, the percentage of broken base pairs remained under 2.6%, indicating that the local order in the system is preserved as the system expands from its initial conformation toward the state captured by the cryo-EM model. When completed, this ambitious simulation will serve as the ultimate test of the accuracy of the MD method.

### A3. Bio-mimetic membrane channel of DNA origami.

Some of the most fascinating biological sensors are membrane protein channels involved in cellular signal transductions. Recently, the function of a membrane channel was reproduced using a novel type of self-assembled DNA structure [33]. The DNA nanochannel was constructed from six dsDNA molecules, featuring a transmembrane pore of  $\sim 2.5$ -nm diameter, see Fig. 3a. To stabilize its placement in a lipid bilayer, hydrophobic ethylthiolate groups were chemically added to phosphate groups that lie inside the lipid bilayer Fig. 3a, mimicking the hydrophobic belt of protein channels. Burns et al. experimentally demonstrated that such DNA channels can conduct ions through otherwise impermeable membranes [33].

We have carried out preliminary MD simulations of a DNA origami membrane channel to characterize its structural fluctuations and the microscopic mechanism of ion conductance [34]. Fig. 3b illustrates the conformation of the simulation system at the end of a 100 ns equilibration trajectory; considerable structural deviations are apparent. The simulation performed under applied electric field characterized the distribution of ions in the channel and the local ionic current densities, Fig. 3c. The flux of  $K^+$  ions was found to determine the total ionic current. The transmembrane bias was also found to produce considerable electroosmotic flow, strongly affecting the translocation of small solutes, such as ATP and ADP.

## List of publications and presentations associated with this work

- M. Shankla and A. Aksimentiev. Conformational transitions and stop-and-go nanopore transport of single-stranded DNA on charged graphene. *Nature Communications*, 5:5171, 2014.
- S. Carson, J. Wilson, A. Aksimentiev, and M. Wanunu. Smooth DNA transport through a narrowed pore geometry. *Biophysical Journal*, 107:2381–2393, 2014.
- M. Belkin, S.-H. Chao, G. Giannetti, and A. Aksimentiev. Modeling thermophoretic effects in solid-state nanopores. *Journal of Computational Electronics*, 13:826–838, 2014.
- S. Banerjee, J. Wilson, J. Shim, M. Shankla, E. A. Corbin, A. Aksimentiev, and R. Bashir. Slowing DNA transport using graphene–DNA interactions. *Advanced Functional Materials*, n/a:n/a–n/a, 2015.
- C.-Y. Li, E. A. Hemmig, J. Kong, J. Yoo, S. Hernández-Ainsa, U. F. Keyser, and A. Aksimentiev. Ionic conductivity, structural deformation and programmable anisotropy of DNA origami in electric field. *ACS Nano*, In revision.
- J. Yoo and A. Aksimentiev. Structural dynamics and ionic conductance of biomimetic DNA origami nanochannels using atomistic molecular dynamics simulations. In preparation, 2015.
- (Presentation) A. Aksimentiev. New Approaches to Sequencing DNA Using a Nanopore. 2014 Pioneer workshop on nanopore and nanofluidics “Physics and application as Biodevices”. Osaka, Japan. February 2014.
- (Presentation) A. Aksimentiev. Reinventing a DNA sequence reader. Distinguished Lecture Series “Nanotechnologies through Materials Innovation”. Northeastern University, Boston. February 2014.
- (Presentation) A. Aksimentiev. Meeting Materials Challenges in Nanopore Sequencing of DNA. CECAM workshop “Simulations of biomolecular interactions with inorganic and organic surfaces as a challenge for future nanotechnologies”. Toulouse, France. March 2014.
- (Presentation) A. Aksimentiev. Engineering DNA Origami Through Microscopic Simulations. Workshop on Origami Engineering. Urbana, IL. April 2014.
- (Presentation) A. Aksimentiev. Molecular Dynamics of DNA origami. Foundations of Nanoscience: Self-Assembled Architectures and Devices (FNANO14). Snowbird, Utah. April 2014.
- (Presentation) A. Aksimentiev. Modeling Nanopores for Sequencing DNA. Gordon Research Conference on Biointerface Science. Lucca (Barga), Italy. June 2014.

- (Poster) C.-Y. Li, J. Yoo, and A. Aksimentiev. Ion Conductivity, Structural Dynamics and the Effective Force in DNA Origami Nanopores. 58th Annual Meeting of the Biophysical-Society San Francisco, CA. FEB 15-19, 2014

## Plan for the next year

For the next year, we plan four individual projects studying DNA origami. The first (P1) is the continuation of the on-going project summarized in Accomplishments A2. The other three (P2, P3, and P4) involve new simulations of DNA origami objects. Specifically, we will explore the possibility of making a nanoscale transistor based on DNA origami (P2). We will reveal the molecular mechanism of DNA origami-based drug delivery vehicles (P3). Finally, we will extend our MD simulation protocol of DNA origami to the next-generation technique, DNA LEGO (P4). Using the NAMD package, we needed to use 80 node hours to perform a 1-ns (NS) simulation of a 1-million-atom (MA) system, 80 NH/MANS. We used this factor to estimate the requested allocation for each project. Projects P1, P2, P3, and P4 will require 108,000, 32,000, 53,000, and 44,000 node hours, respectively, resulting in the **total requested allocation of 238,000 node hours**. P1 will be finished during Q1. The other three projects will be performed during Q2.

In case we are allowed to use unused allocations by other BW professors, we will design DNA origami channels that have functionality of biological ion channel (P5). This project will require **additional 76,800 node hours**, and will be performed during Q3.

**P1. Direct comparison with the results of cryo-EM reconstruction.** We will continue the simulation in Accomplishments A2 to finish the project. Currently, we have performed the simulation for 50 ns. Based on our previous MD simulations [21] and the RMSD plot in Fig. 2b, we expect the equilibration will be finished in an additional 50 ns. Using the equilibrated system, we will perform a production run for 200 ns that will reveal the equilibrium structure and the dynamics of the DNA helices. In our previous simulations of a rod-like structure of 4-by-4 DNA helices [21], which had a similar design but roughly one order of magnitude smaller cross-sectional area, we showed that a 100-ns production run is long enough to sample local structural fluctuation. The system contains 6.75 million atoms. This project will require  $80 \text{ NH/MANS} \times 6.75 \text{ million atoms} \times 200 \text{ ns} = 108,000$  node hours.

**P2. DNA origami transistor.** Can we make a transistor out of DNA origami? The results of our preliminary simulations suggest that this might be possible. We have found that the distance between the layers of a DNA origami plate can be reversibly changed by switching on and off an applied electric field directed normal to the plate, Fig. 4a. The motion of the helices alters the number of ions gathered within the DNA origami structure and the ion mobility. Such a change in the number and mobility of charge carriers should affect the conductance of the DNA origami along its helical direction. Preliminary simulations of the ionic current flowing through a bundle of 64 dsDNA helices confined to a cylinder of a given radius have confirmed this assessment: the ionic current along the DNA bundle increases with the average distance between the DNA molecules in the bundle, Fig. 4b. We will carry out a proof-of-principle demonstration of a DNA origami transistor using a system of two intersecting channels. A DNA origami structure will be placed at the

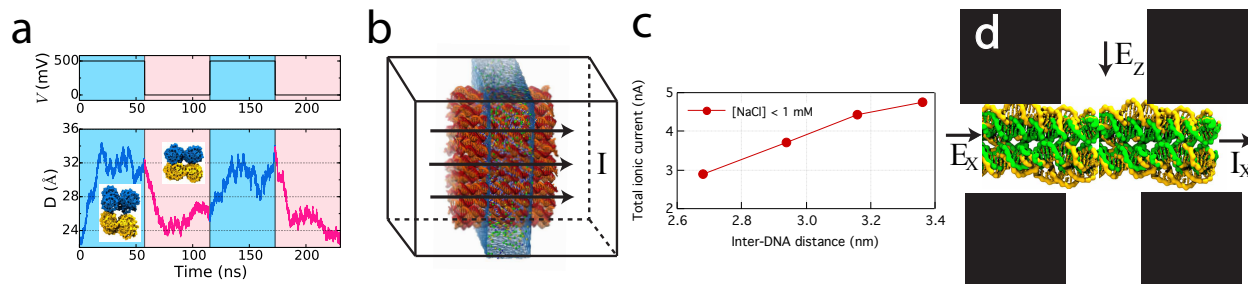


Figure 4: DNA origami transistor. (a) External electric bias modulates the distance between the layers of a DNA origami plate [22]. (b) MD simulation of a bundle of 64 dsDNA helices (red and orange) subject to an external electric field [35]. (c) Ionic current along the DNA bundle shown in panel b depends on the average DNA-DNA distance in the bundle. (d) Schematics of a DNA origami transistor. A DNA origami structure is placed at the intersection of two nanochannels. The magnitude of the electric field along the vertical channel,  $E_z$  modulates the distance between the layers in the DNA origami structure (see also panel a). Expansion and contraction of the origami modulates the ionic current along the origami,  $I_x$  (see also panel c).

junction of the channels, Fig. 4d. An electric field applied across the DNA origami and the electroosmotic flow induced by the field will modulate the spacing between the DNA helices. We will examine how the resultant swelling or shrinking of the origami structure gates the ionic current flowing through the channel containing the origami structure. The system will contain  $\sim 0.2$  million atoms. The typical time scale for the expansion and contraction of the DNA origami plates induced by the normal electric field was  $\sim 200$  ns in our previous simulations [22]. Thus, a contraction-expansion cycle will require 400 ns. We will repeat this cycle five times to test reproducibility. This project will require  $80 \text{ NH/MANS} \times 0.2 \text{ million atoms} \times 2,000 \text{ ns} = 32,000 \text{ node hours}$ .

**P3. DNA origami box for drug delivery.** We will simulate a reversibly switchable DNA origami box that was recently reported by Zadegan *et al.* [36]. The size of Zadegan’s DNA origami box was  $18 \times 18 \times 24 \text{ nm}^3$ , Fig. 5. We have already built an all-atom structure of this DNA origami box. After allowing  $\sim 4\text{-nm}$  gap between the box and its periodic images, the final dimensions of the system are  $22 \times 22 \times 28 \text{ nm}^3$ , containing 1,350,000 atoms. Using this equilibrated system, we will perform two different simulations to reveal how this DNA box works on the molecular level. First, we will test how many drug molecules can be loaded to the origami box. When loaded, drugs contained within the DNA origami box will exert an osmotic pressure on the box that may limit the concentration of drugs that can be held within. To ensure that the box is stable even when loaded with a high concentration of drugs, we will insert drug molecules into the equilibrated box and simulate the resulting system for 100 ns. Second, we will characterize the conformational change in the box in the process of opening, Fig. 5. The DNA origami box designed by Zadegan *et al.* [36] can open and close by introducing a single-stranded DNA “key”. To open the box, the ssDNA key is introduced which alters DNA strands that specifically keep the lid closed. These strands are then in their “unlocked” state and the hinged lid is free to diffuse to its open conformation. Although it would be too expensive to simulate the “unlocking” strand exchange process or drugs exiting the box, we will investigate whether the box will open reliably after it is unlocked. Based on the diffusion speed of the macromolecule in solution, we estimate that 400 ns is necessary to

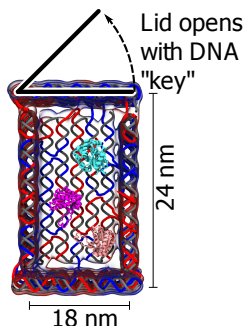


Figure 5: Illustration of the DNA origami box for drug delivery containing drug molecules and the proposed opening of the lid [36].

observe a significant opening event. This project will require  $80 \text{ NH/MANS} \times 1.35 \text{ million atoms} \times 500 \text{ ns} = 54,000 \text{ node hours}$ .

**P4. Structure and conductivity of DNA bricks.** The most recently discovered DNA origami-like approach, is the DNA brick technique [37]. This technique allows us to build various objects using a subset of a predefined library, in a similar way to LEGO. To investigate the feasibility of using DNA brick structures for nanopore sensing, we will first build an atomic-scale model of a fully filled cube with  $\sim 15\text{-nm}$ -long edges [37]. The structure will then be solvated and simulated using the MD method in the absence of an external electric field to determine its equilibrium conformation and the extent of structural fluctuations. Although the assembled DNA LEGO structure is similar to the square lattice DNA origami, we expect the former to have different mechanical properties because of the shorter length of the DNA strands (32-nt oligomers vs. long scaffold strand) and a different crossover pattern (double crossovers vs. single crossover). Once the characterization of structural and mechanical properties is completed, we will measure the ionic permeability of the DNA LEGO plates under various applied biases when placed upon a solid-state nanocapillary and when in solution. The simulations will assess the suitability of DNA bricks structures for nanopore measurements, uncovering new avenues for improving their design. The system will contain  $\sim 0.5$  million atoms. For the equilibrium simulation, we estimate that 200 ns is necessary based on our previous simulation, [21]. For the simulations of ionic permeabilities, we will use three different biases (100, 200, and 400 mV) on a solid-state nanocapillary or in solution; each simulation will require a 150-ns simulation to obtain statistically converged ionic currents [22]. The total simulation time will be  $200 \text{ ns} + 6 \times 150 \text{ ns} = 1,100 \text{ ns}$ . This project will require  $80 \text{ NH/MANS} \times 0.5 \text{ million atoms} \times 1,100 \text{ ns} = 44,000 \text{ node hours}$ .

**P5. (Optional) Rational design of ion-selective or voltage-sensing DNA origami ion channels.**

In case we are allowed to use unused allocations by other BW professors, we will attempt to design DNA origami channels with either ion selectivity or voltage-sensitivity using MD methods. See Fig. 6 for the schematic illustrations of those channels. Our successful designs will be experimentally validated by the Keyser group (Cambridge, UK). To mimic the ion-selectivity filter or voltage-sensing domains in membrane channel proteins, we will add similar functional groups to the DNA channels reported in Achievements A3, Fig. 6a,b. When we introduce new functional groups in the channel system, we will need to equilibrate the system for  $\sim 100 \text{ ns}$ . Then, a 100-ns simulation with a 200-mV bias will be followed to characterize the effect of the introduced functional groups on the ionic current through the channel. We will try 20 different functional groups. The system will contain  $\sim 0.24$  million atoms. This project will require  $80 \text{ NH/MANS} \times 0.24 \text{ million atoms} \times 200 \text{ ns per functional group} \times 20$

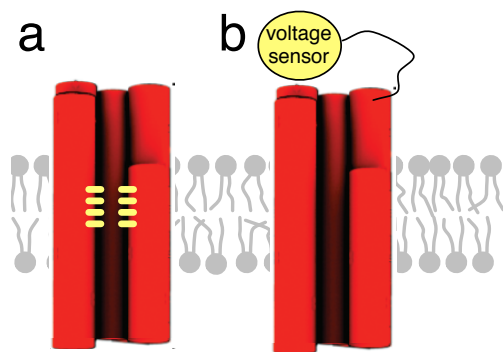


Figure 6: (a) A schematic illustration of a DNA origami channel (red cylinders) with a selectivity filter (yellow marks). (b) A schematic illustration of a DNA origami channel with a charged voltage sensing domain (yellow sphere).

functional groups = 76,800 node hours.

## References

- [1] N. C. Seeman. Nanomaterials based on DNA. *Annual Review of Biochemistry*, 79:65–87, 2010.
- [2] A. V. Pinheiro, D. Han, W. M. Shih, and H. Yan. Challenges and opportunities for structural DNA nanotechnology. *Nature Nanotechnology*, 6:763–72, 2011.
- [3] P. W. K. Rothemund. Folding DNA to create nanoscale shapes and patterns. *Nature*, 440:297–302, 2006.
- [4] S. M. Douglas, H. Dietz, T. Liedl, B. Högberg, F. Graf, and W. M. Shih. Self-assembly of DNA into nanoscale three-dimensional shapes. *Nature*, 459:414–8, 2009.
- [5] H. Dietz, S. M. Douglas, and W. M. Shih. Folding DNA into twisted and curved nanoscale shapes. *Science*, 325:725–30, 2009.
- [6] D. Han, S. Pal, J. Nangreave, Z. Deng, Y. Liu, and H. Yan. DNA origami with complex curvatures in three-dimensional space. *Science*, 332:342–6, 2011.
- [7] E. S. Andersen, M. Dong, M. M. Nielsen, K. Jahn, R. Subramani, W. Mamdouh, M. M. Golas, B. Sander, H. Stark, C. L. P. Oliveira, J. S. Pedersen, V. Birkedal, F. Besenbacher, K. V. Gothelf, and J. Kjems. Self-assembly of a nanoscale DNA box with a controllable lid. *Nature*, 459:73–6, 2009.
- [8] T. Liedl, B. Högberg, J. Tytell, D. E. Ingber, and W. M. Shih. Self-assembly of three-dimensional prestressed tensegrity structures from DNA. *Nature Nanotechnology*, 5:520–4, 2010.
- [9] C. Lin, R. Jungmann, A. M. Leifer, C. Li, D. Levner, G. M. Church, W. M. Shih, and P. Yin. Submicrometre geometrically encoded fluorescent barcodes self-assembled from DNA. *Nature Chemistry*, 4:832–839, 2012.
- [10] J.-P. J. Sobczak, T. G. Martin, T. Gerling, and H. Dietz. Rapid folding of DNA into nanoscale shapes at constant temperature. *Science*, 338:1458–61, 2012.

- [11] M. Langecker, V. Arnaut, T. G. Martin, J. List, S. Renner, M. Mayer, H. Dietz, and F. C. Simmel. Synthetic lipid membrane channels formed by designed DNA nanostructures. *Science*, 338:932–6, 2012.
- [12] G. P. Acuna, F. M. Möller, P. Holzmeister, S. Beater, B. Lalkens, and P. Tinnefeld. Fluorescence enhancement at docking sites of DNA-directed self-assembled nanoantennas. *Science*, 338:506–10, 2012.
- [13] A. Kuzyk, R. Schreiber, Z. Fan, G. Pardatscher, E.-M. M. Roller, A. Högele, F. C. Simmel, A. O. Govorov, and T. Liedl. DNA-based self-assembly of chiral plasmonic nanostructures with tailored optical response. *Nature*, 483:311–4, 2012.
- [14] D. J. Kauert, T. Kurth, T. Liedl, and R. Seidel. Direct mechanical measurements reveal the material properties of three-dimensional DNA origami. *Nano Letters*, 11:5558–5563, 2011.
- [15] X.-C. C. Bai, T. G. Martin, S. H. W. Scheres, and H. Dietz. Cryo-EM structure of a 3D DNA-origami object. *Proceedings of the National Academy of Sciences, USA*, 109:20012–7, 2012.
- [16] D.-N. Kim, F. Kilchherr, H. Dietz, and M. Bathe. Quantitative prediction of 3D solution shape and flexibility of nucleic acid nanostructures. *Nucleic Acids Research*, 2011.
- [17] K. Pan, D.-N. N. Kim, F. Zhang, M. R. Adendorff, H. Yan, and M. Bathe. Lattice-free prediction of three-dimensional structure of programmed DNA assemblies. *Nature Communications*, 5:5578, 2014.
- [18] T. E. Ouldridge, A. A. Louis, and J. P. K. Doye. Structural, mechanical, and thermodynamic properties of a coarse-grained DNA model. *The Journal of Chemical Physics*, 134:085101, 2011.
- [19] T. E. Ouldridge, R. L. Hoare, A. A. Louis, J. P. K. Doye, J. Bath, and A. J. Turberfield. Optimizing dna nanotechnology through coarse-grained modeling: a two-footed dna walker. *ACS Nano*, 7:2479–90, 2013.
- [20] C. Maffeo, T. T. M. Ngo, T. Ha, and A. Aksimentiev. A coarse-grained model of unstructured single-stranded DNA derived from atomistic simulation and single-molecule experiment. *Journal of Chemical Theory and Computation*, 10:2891–2896, 2014.
- [21] J. Yoo and A. Aksimentiev. In situ structure and dynamics of DNA origami determined through molecular dynamics simulations. *Proceedings of the National Academy of Sciences, USA*, 110:20099–20104, 2013.
- [22] C.-Y. Li, E. A. Hemmig, J. Kong, J. Yoo, S. Hernández-Ainsa, U. F. Keyser, and A. Aksimentiev. Ionic conductivity, structural deformation and programmable anisotropy of DNA origami in electric field. Submitted.

- [23] M. Shankla and A. Aksimentiev. Conformational transitions and stop-and-go nanopore transport of single-stranded DNA on charged graphene. *Nature Communications*, 5:5171, 2014.
- [24] S. Carson, J. Wilson, A. Aksimentiev, and M. Wanunu. Smooth DNA transport through a narrowed pore geometry. *Biophysical Journal*, 107:2381–2393, 2014.
- [25] S. Banerjee, J. Wilson, J. Shim, M. Shankla, E. A. Corbin, A. Aksimentiev, and R. Bashir. Slowing DNA transport using graphene–DNA interactions. *Advanced Functional Materials*, n/a:n/a–n/a, 2015.
- [26] M. Belkin, S.-H. Chao, G. Giannetti, and A. Aksimentiev. Modeling thermophoretic effects in solid-state nanopores. *Journal of Computational Electronics*, 13:826–838, 2014.
- [27] A. Aksimentiev and K. Schulten. Imaging alpha-hemolysin with molecular dynamics: Ionic conductance, osmotic permeability and the electrostatic potential map. *Biophysical Journal*, 88:3745–3761, 2005.
- [28] N. A. W. Bell, C. R. Engst, M. Ablay, G. Divitini, C. Ducati, T. Liedl, and U. F. Keyser. DNA origami nanopores. *Nano Letters*, 12:512–517, 2012.
- [29] R. Wei, T. G. Martin, U. Rant, and H. Dietz. DNA origami gatekeepers for solid-state nanopores. *Angewandte Chemie International Edition*, 51:4864–7, 2012.
- [30] S. Hernández-Ainsa, N. A. W. Bell, V. V. Thacker, K. Göpfrich, K. Misiunas, M. E. Fuentes-Perez, F. Moreno-Herrero, and U. F. Keyser. DNA origami nanopores for controlling DNA translocation. *ACS Nano*, 7:6024–6030, 2013.
- [31] S. Hernández-Ainsa, K. Misiunas, V. V. Thacker, E. A. Hemmig, and U. F. Keyser. Voltage-Dependent Properties of DNA Origami Nanopores. *Nano Letters*, 14:1270–1274, 2014.
- [32] B. Luan and A. Aksimentiev. Electro-osmotic screening of the DNA charge in a nanopore. *Physical Review E*, 78:021912, 2008.
- [33] J. R. Burns, E. Stulz, and S. Howorka. Self-assembled DNA nanopores that span lipid bilayers. *Nano Letters*, 13:2351–2356, 2013.
- [34] J. Yoo and A. Aksimentiev. Structural dynamics and ionic conductance of biomimetic DNA origami nanochannels using atomistic molecular dynamics simulations. In preparation.
- [35] J. Yoo and A. Aksimentiev. Improved parametrization of  $\text{Li}^+$ ,  $\text{Na}^+$ ,  $\text{K}^+$ , and  $\text{Mg}^{2+}$  ions for all-atom molecular dynamics simulations of nucleic acid systems. *Journal of Physical Chemistry Letters*, 3:45–50, 2012.
- [36] R. M. Zadegan, M. D. E. Jepsen, K. E. Thomsen, A. H. Okholm, D. H. Schaffert, E. S. Andersen, V. Birkedal, and J. Kjems. Construction of a 4 zeptoliters switchable 3D DNA box origami. *ACS Nano*, 6:10050–10053, 2012.

- [37] Y. Ke, L. L. . L. Ong, W. M. . M. Shih, and P. Yin. Three-dimensional structures self-assembled from DNA bricks. *Science*, 338:1177–1183, 2012.